

# Rate-Maximizing OFDM Pilot Patterns for UAV Communications in Nonstationary A2G Channels

Raghunandan M. Rao\*, Vuk Marojevic\*, Jeffrey H. Reed\*

\*Bradley Department of Electrical and Computer Engineering

Virginia Tech, Blacksburg, Virginia, USA

Email: {raghumr, maroje, reedjh}@vt.edu

**Abstract**—In this paper, we propose and evaluate rate-maximizing pilot configurations for Unmanned Aerial Vehicle (UAV) communications employing OFDM waveforms. OFDM relies on pilot symbols for effective communications. We formulate a rate-maximization problem in which the pilot spacing (in the time-frequency resource grid) and power is varied as a function of the *time-varying channel statistics*. The receiver solves this rate-maximization problem, and the optimal pilot spacing and power are *explicitly fed back* to the transmitter to adapt to the time-varying channel statistics in an air-to-ground (A2G) environment. We show the enhanced throughput performance of this scheme for UAV communications in sub-6 GHz bands. These performance gains are achieved at the cost of very low computational complexity and feedback requirements, making it attractive for A2G UAV communications in 5G.

**Index Terms**—UAV Communications, Rate Maximization, Adaptive Pilot Patterns, Channel Statistics Codebook.

## I. INTRODUCTION

Unmanned Aerial Vehicle (UAV) communications has spurred a lot of interest in recent years, in particular due to an upsurge in its wide-ranging applications such as Internet by drones, package delivery and public safety networks. The Third Generation Partnership Project (3GPP) has frozen Release 15 in December 2017, which publishes the first specifications for 5G New Radio (5G NR). Integrating UAVs with 5G is one of the most promising approaches being considered to facilitate ubiquitous high speed as well as low latency communications.

Maintaining a high spectral efficiency in the face of impending densification of UAVs will be challenging in the future, particularly in the crowded sub-6 GHz bands. Moreover, the channel statistics of air-to-ground channels will be significantly different than those of terrestrial wireless channels. For instance, UAV communications operate in a Line of Sight (LoS) or near-LoS environments, unlike the rich scattering multipath environments observed in terrestrial channels. Moreover, high mobility UAV scenarios such as package delivery, mission-specific military drones etc. will experience fast temporal fading due to Doppler shifts. Since 5G is anticipated to encompass a wide variety of channel

scenarios, it is more efficient to allow for self-optimization in order to adapt to time-varying channel environments.

Xue et al. [1] present joint time-frequency scheduling and power allocation schemes to manage the effect of channel fading and adjacent channel interference in multi-UAV communications. He et al. [2] optimize the UAV's altitude and antenna beamwidth, coupled with a fly-hover-and-communicate protocol to efficiently serve ground terminals partitioned into disjoint clusters. Jaber et al. [3] optimize OFDM parameters as a function of carrier frequency and UAV speed or type.

In modern wireless standards, pilots are used for coherent demodulation and channel state information (CSI) estimation. Current wireless standards employ fixed pilot configurations that are designed for the worst-case channel conditions. With 4G LTE, the pilot pattern was primarily designed for terrestrial communications. However, this is clearly not the case for UAV communications in LoS and potentially fast fading A2G channels. Fig. 1 illustrates how the pilot spacing can be changed as a function of the Doppler and delay spreads to balance pilot overhead with channel estimation accuracy.

Whereas most of the recent literature has focused on nearly static channel conditions or low-speed UAVs, we develop a methodology for optimizing pilot signal configurations to maximize rate for UAVs in A2G channels with time-varying statistics, specifically, Doppler spread and delay spread. As [4] and [5] have shown, the rate-maximizing pilot pattern is a function of the time-frequency fading characteristics, and the operating SNR of the channel. Although 5G NR allows varying the pilot density in the time domain, (a) it has a limited number of configurations, and (b) it does not allow changing pilot density in the frequency domain [6], which limits resources for data in LoS A2G channels.

Our approach follows the principles of [5]. We compare the throughput performance of our proposed rate-maximizing pilot scheme against other fixed pilot configurations in a *realistic A2G channel with time-varying statistics*. We also explore explicit feedback mechanisms to facilitate dynamic pilot adaptation. This is opposed to implicit feedback, which was introduced in [5]. We observe that signaling overhead for explicit feedback is negligible, and is of the same order of magnitude as implicit feedback, with low computational complexity.

The rest of the paper is organized as follows: Section II formulates the optimization problem for finding rate-maximizing

This is the author's version of the work. For citation purposes, the definitive version of record of this work is: R. M. Rao, V. Marojevic and J. H. Reed, "Rate-Maximizing OFDM Pilot Patterns for UAV Communications in Nonstationary A2G Channels," *To Appear in the 88th IEEE Vehicular Technology Conference (IEEE VTC Fall 2018)*, pp. 1– 5, August 2018.

pilot patterns. Section III introduces the channel statistics codebook, and discusses the feedback mechanisms to enable pilot adaptation. Section IV provides numerical results and analysis comparing our adaptive rate-maximizing pilot design with that of fixed pilot configurations. Section V concludes the paper.

## II. PROBLEM FORMULATION AND SYSTEM MODEL

### A. Rate-Maximizing Pilot Configurations

Finding the optimal pilot configuration can be formulated as a maximization problem of the upper bound of the achievable rate [4], [5], which can be written as

$$\begin{aligned} & \underset{\{\rho, \Delta_{pf}, \Delta_{pt}\}}{\text{maximize}} && S(\Delta_{pf}, \Delta_{pt}) \cdot \log_2(1 + \bar{\gamma}) \\ & \text{subject to} && \bar{P}(\rho, \Delta_{pf}, \Delta_{pt}) \leq 1 \\ & && 1 \leq \Delta_{pt} \leq T_{max} \\ & && 2 \leq \Delta_{pf} \leq F_{max} \\ & && \rho_{min} \leq \rho \leq \rho_{max}, \end{aligned} \quad (1)$$

where  $\Delta_{pt}$  and  $\Delta_{pf}$  are the pilot spacing in time and frequency. The average data-to-pilot power ratio is given by  $\rho = \sigma_d^2 / \sigma_p^2$ . The triad  $\mathcal{V} = \{\rho, \Delta_{pf}, \Delta_{pt}\}$  completely describes the pilot configuration. The upper limits on pilot spacing in time and frequency is given by  $T_{max}$  and  $F_{max}$  respectively, which is found using sampling considerations [7]. The average power per resource element is given by  $\bar{P}(\mathcal{V})$ , which is a function of the pilot configuration as shown in [5]. The upper (lower) limit on  $\rho$  is denoted by  $\rho_{max}$  ( $\rho_{min}$ ) respectively. The average post-equalization SINR ( $\bar{\gamma}$ ) for a zero-forcing (ZF) receiver can be written as

$$\bar{\gamma} = \frac{\sigma_d^2 \cdot \sigma_{ZF}}{\sigma_w^2 + \sigma_{ICI}^2 + \sigma_{MSE}^2 \cdot \sigma_d^2}, \quad (2)$$

where  $\sigma_d^2$  ( $\sigma_p^2$ ) is the average power per data (pilot) symbol,  $\sigma_w^2$  the noise power and  $\sigma_{ZF} = 1$  for a  $M \times M$ -MIMO system [4]. The channel estimation mean squared error (MSE) is given by  $\sigma_{MSE}^2$ , which can be computed using the expressions derived in [4], [5]<sup>1</sup>. It is important to note that  $\sigma_{MSE}^2$  is a function of the channel's temporal correlation  $R_t(\Delta t)$ , spectral correlation  $R_f(\Delta f)$  and the average pilot SNR ( $\sigma_p^2 / \sigma_w^2$ ). The intercarrier interference  $\sigma_{ICI}^2$  is assumed to be dominated by user mobility in the vehicular network and can be estimated using [8]

$$\sigma_{ICI}^2 \leq \frac{1}{3} \left( \frac{\pi f_d \sigma_d}{\Delta f} \right)^2, \quad (3)$$

where  $f_d$  is the maximum Doppler shift and  $\Delta f$  the subcarrier spacing. The spectrum utilization function  $S(\Delta_{pf}, \Delta_{pt})$  is simply the fraction of data REs in the OFDM grid across all layers over the total number of REs, and can be easily computed with the knowledge of  $\mathcal{V}$ . Additional control channels and signals are ignored here without loss of generality.

<sup>1</sup>The channel estimation MSE has been derived for 'diamond-shaped' pilot patterns in [4], [5]. Note that this pattern is used in modern cellular standards such as LTE and NR.  $\sigma_{MSE}^2$  for other frequency/time comb patterns can be derived in a similar manner.

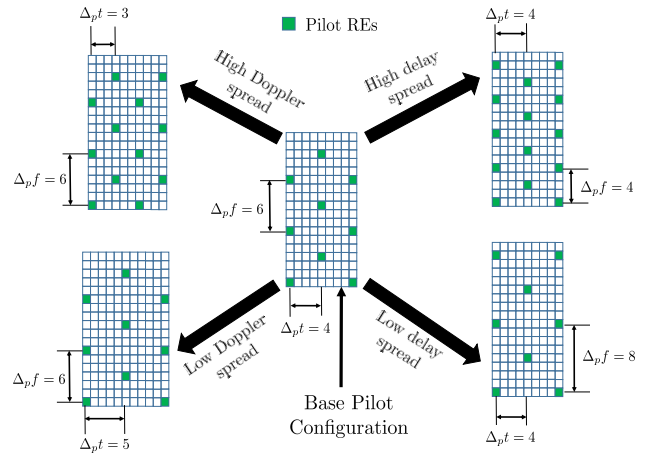


Fig. 1: Illustration of pilot parameter adaptation in the OFDM resource grid as a function of channel statistics.

In order to estimate the achievable rate as a function of  $\mathcal{V}$ , the unknown quantities that need to be estimated are  $\sigma_{MSE}^2$ ,  $f_d$  and  $\sigma_w^2$ .

Noise power can be estimated using the methods proposed in [9]. To estimate the channel statistics  $\hat{R}_t(\Delta t)$  and  $\hat{R}_f(\Delta f)$  in a nonstationary vehicular environment, temporal averaging can be performed assuming local stationarity [5], [10], [11]. With the estimated channel matrix  $\hat{\mathbf{H}} \in \mathbb{C}^{N_{sub} \times T_{ofdm}}$ , the channel correlation can be estimated using

$$\begin{aligned} \hat{R}_t(-i) &= \frac{1}{T_{ofdm} - |i|} \sum_{t=1}^{T_{ofdm} - |i|} \left\{ \text{diag}_i \left[ \hat{\mathbf{H}}^H \hat{\mathbf{H}} \right] \right\}_t \\ \hat{R}_f(-j) &= \frac{1}{N_{sub} - |j|} \sum_{f=1}^{N_{sub} - |j|} \left\{ \text{diag}_j \left[ \hat{\mathbf{H}} \hat{\mathbf{H}}^H \right] \right\}_f, \end{aligned} \quad (4)$$

where  $N_{sub}$  is the number of subcarriers and  $T_{ofdm}$  the number of OFDM symbols in the channel statistics estimation window. The term  $\text{diag}_i[\mathbf{X}]$  is the vectorized  $i^{\text{th}}$  diagonal of matrix  $\mathbf{X}$ , and  $\left\{ \text{diag}_i[\mathbf{X}] \right\}_k$  its  $k^{\text{th}}$  element. Due to conjugate symmetry, the other elements can be found using  $\hat{R}_t(-i) = \hat{R}_t^*(i)$  and  $\hat{R}_f(-j) = \hat{R}_f^*(j)$ . This formulation can be extended to MIMO-OFDM, where the channel spectral and temporal correlation is estimated for each layer<sup>2</sup>.

## III. PRACTICAL CHANNEL STATISTICS ESTIMATION AND FEEDBACK

In practical scenarios where the channel statistics are estimated over a finite duration, the accuracy will degrade due to (a) interpolation errors, and (b) addition of noise. In the worst case, the estimated channel statistics can violate the properties of the autocorrelation function  $|\hat{R}_t(\Delta t)| \leq \hat{R}_t(0) \forall \Delta t \neq 0$ . This can happen especially in high noise, low mobility and/or flat fading scenarios. Using these estimated channel statistics

<sup>2</sup>Typically the spectral and temporal correlation is the same for the channel between each tx-rx antenna pair, unless the antennas are distributed in different locations of the network.

directly can result in inconsistent, and sometimes absurd values for the MSE. We propose a codebook-based approach to mitigate this issue, as well as reduce feedback requirements.

### A. Channel Statistics Codebook

We propose a codebook that contains a finite number of channel statistics, i.e. channel correlations in the time and frequency dimensions. Let the codebook be denoted by set  $\mathcal{R}_C$  with two sets  $\mathcal{R}_{C,t} \in \mathcal{R}_C$  and  $\mathcal{R}_{C,f} \in \mathcal{R}_C$ . Let  $|\mathcal{R}_{C,f}| = M_f$  and  $|\mathcal{R}_{C,t}| = M_t$ , where  $|\cdot|$  denotes the cardinality of a set.  $\mathcal{R}_{C,f}$  is the set of channel frequency correlation profiles with vector elements  $\mathbf{R}_{fc,l} \in \mathcal{R}_{C,f}, 1 \leq l \leq M_f$ . Likewise,  $\mathcal{R}_{C,t}$  is the set of channel temporal correlation profiles with vector elements  $\mathbf{R}_{tc,m} \in \mathcal{R}_{C,t}, 1 \leq m \leq M_t$ . Here, we model temporal fading using a classic Doppler spectrum where the  $(\Delta t)^{th}$  element of  $\mathbf{R}_{tc,m}$  is  $[\mathbf{R}_{tc,m}]_{\Delta t} = J_0(2\pi f_{d,m}\Delta t)$ , with  $f_{d,m}$  being the maximum Doppler frequency for the  $m^{th}$  temporal correlation profile. This codebook design is motivated by the Wide sense stationary uncorrelated scattering (WSSUS) approximation, which allows for independent modeling of multipath fading and user mobility. In general, codebook elements of  $\mathcal{R}_{C,f}$  ( $\mathcal{R}_{C,t}$ ) is a vector of length  $N_{\Delta t}$  ( $N_{\Delta f}$ ) respectively. The vector lengths  $N_{\Delta t}$  and  $N_{\Delta f}$  must be chosen to balance accuracy of channel correlation estimation and computational complexity. For the sake of representation  $\mathcal{R}_{C,t}$  ( $\mathcal{R}_{C,f}$ ) can be parametrized by  $f_d$  ( $\tau_{rms}$ ) respectively, as shown in Table II.

### B. Estimation and Feedback of Optimal Parameters

In order to reliably communicate, the transmitter and receiver should share  $\{\mathcal{P}, \mathcal{D}_f, \mathcal{D}_t\}$ , which are the sets for  $\{\rho, \Delta_p f, \Delta_p t\}$  respectively. Using (1), Algorithm 1 finds  $\mathcal{V}_o$  and updates it every  $T_{ofdm}$  symbols. For small discrete-valued feasible sets, a simple brute force method to find  $\mathcal{V}_o$  is practically feasible. The receiver feeds back  $\mathcal{V}_o$ , which is then used by the transmitter for transmission for the next  $T_{ofdm}$  OFDM symbols. Fig. 2 shows the processing and feedback of codebook indices for pilot adaptation. The computational complexity of Algorithm 1 is low since it is composed of matrix multiplication operations and optimization problems involving discrete-valued, low-dimensional feasible sets.

### C. Feedback Mechanisms and Requirements

Here we discuss two methods for feeding back the optimal pilot configuration.

1) *Explicit Feedback of the Optimal Parameters*: The receiver can use explicit feedback of the the optimal parameters  $\mathcal{V}_o$  to facilitate pilot adaptation as shown in Fig. 2. In this case, the minimum number of bits required will be  $b_{exp}^{(fb)} = \lceil \log_2(M_{\mathcal{P}}M_{\mathcal{D}_f}M_{\mathcal{D}_t}) \rceil$  bits, where  $M_{\mathcal{P}} = |\mathcal{P}|$ ,  $M_{\mathcal{D}_f} = |\mathcal{D}_f|$  and  $M_{\mathcal{D}_t} = |\mathcal{D}_t|$ . Since the codebook indices are fed back once every  $(T_{ofdm}T_s)$  seconds, the rate overhead for explicit feedback will be  $R_{exp}^{(fb)} = b_{exp}^{(fb)} / (T_{ofdm}T_s)$  bps.

### Algorithm 1 Pilot Adaptation using Explicit Feedback: Receiver Processing and Signaling

**Input:** Codebook  $\mathcal{R}_C$  and  $\{\mathcal{D}_f, \mathcal{D}_t$  and  $\mathcal{P}\}$ .

- 1: Estimate  $\hat{R}_t$  and  $\hat{R}_f$  from equation (4) using  $\hat{\mathbf{H}}$ , computed using the most recent  $T_{ofdm}$  OFDM symbols.
- 2: Find  $\mathbf{R}_{fc,l'} \in \mathcal{R}_{C,f}$  and  $\mathbf{R}_{tc,m'} \in \mathcal{R}_{C,t}$  by solving

$$l' = \arg \min_{1 \leq l \leq M_f} \|\hat{\mathbf{R}}_f - \mathbf{R}_{fc,l}\|$$

$$m' = \arg \min_{1 \leq m \leq M_t} \|\hat{\mathbf{R}}_t - \mathbf{R}_{tc,m}\|. \quad (5)$$

- 3: For all allowed values of  $\mathcal{V} = \{\rho, \Delta_p f, \Delta_p t\} \in \{\mathcal{P}, \mathcal{D}_f, \mathcal{D}_t\}$ , compute  $\sigma_{MSE}^2$  (see [5]).
- 4: For all allowed values of  $\mathcal{V}$ , solve equation (5) to obtain the optimal parameters  $\mathcal{V}_o = \{\rho_o, (\Delta_p f)_o, (\Delta_p t)_o\}$ .
- 5: Feed back the optimal parameter set  $\mathcal{V}_o$ .
- 6: For the next  $T_{ofdm}$  OFDM symbols, use  $\mathcal{V}_o$  to estimate the new channel matrix  $\hat{\mathbf{H}} \in \mathbb{C}^{N_{sub} \times T_{ofdm}}$ .
- 7: Go back to step 1.

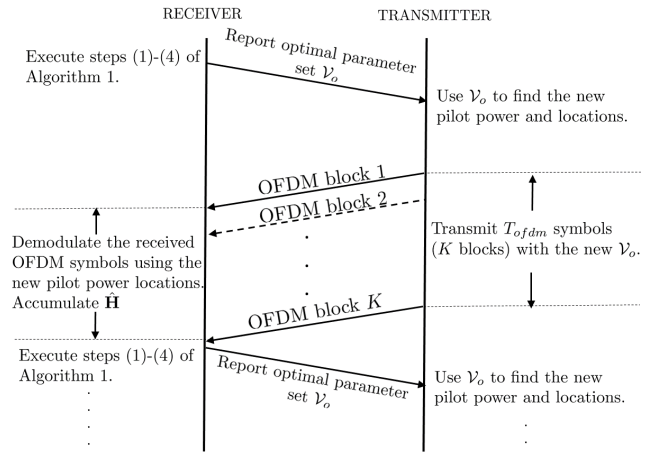


Fig. 2: Illustration of the explicit feedback of pilot parameters between the transmitter and the receiver based on Algorithm 1.  $K$  OFDM blocks are equivalent to  $T_{ofdm}$  OFDM symbols.

2) *Implicit Feedback using Codebook Indices*: If the cardinality of the feasible set is large, the feedback requirements can be further reduced by implicit feedback, where the codebook indices  $(l', m')$  are fed back instead of  $\mathcal{V}_o$ . In this case, the minimum number of bits required is  $b_{imp}^{(fb)} = \lceil \log_2(M_t M_f) \rceil$  bits. The rate overhead for implicit feedback will be  $R_{imp}^{(fb)} = b_{imp}^{(fb)} / (T_{ofdm}T_s)$  bps.

## IV. NUMERICAL RESULTS

We consider a A2G wireless channel in the 5 GHz band. The wireless channel can be parametrized by the signal-to-noise ratio (SNR), Doppler spread ( $f_d$ ) and the root-mean squared (r.m.s.) delay spread ( $\tau_{rms}$ ). To model the wireless channel, we used the tapped-delay line model with a time-varying power delay profile (PDP) and the Jakes Doppler spectrum applied on each multipath component with the appropriate  $f_d$ .

Although a channel with time varying statistics is nonstationary, the channel can be approximated to be stationary

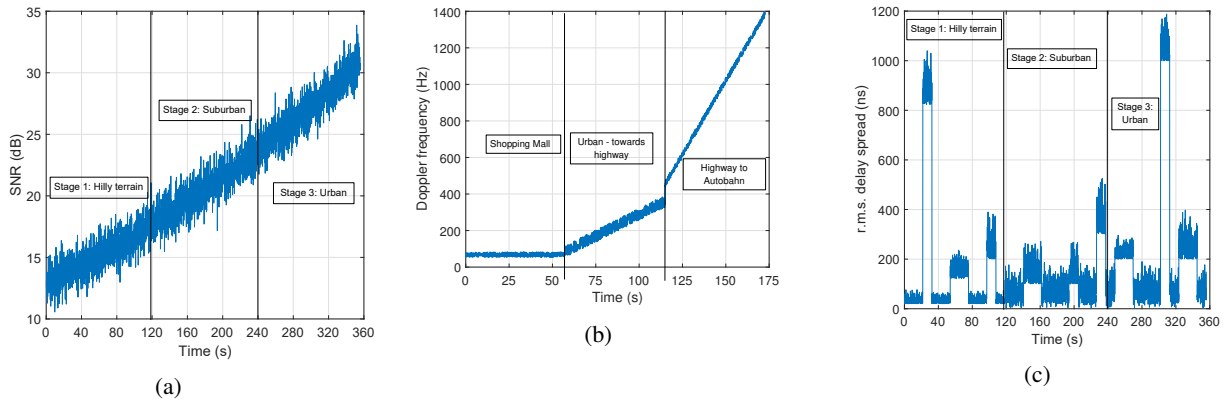


Fig. 3: Variation of (a) SNR, (b)  $f_d$  and (c)  $\tau_{rms}$  over time in the simulation scenario.

TABLE I: Simulation Parameters

Parameter	Value
Antenna Configuration	SISO
FFT-length	128
No. of subcarriers ( $N_{sub}$ )	72
Center Frequency ( $f_c$ )	5 GHz
Subcarrier Spacing ( $\Delta f$ )	15 kHz
OFDM symbol duration ( $T_s$ )	71.875 $\mu s$
Cyclic Prefix Duration	5.21 $\mu s$
Base pilot spacing	$\Delta_p t = 4$ (0.2875 ms) $\Delta_p f = 6$ (90 kHz)
Channel parameters	Doubly selective: Jakes Doppler spectrum with multipath fading.
Transmit power	37.5 dBm
Noise Power Spectral Density	-174 dBm/Hz
Pathloss parameters [10]	$A = 116$ dB, $n = 1.8$ , $\sigma_X = 3.1$ dB $F = 2.3$ dB, $R_{max} = 19$ km $R_{min} = 1.7$ km
Channel Estimation	Least Squares (pilots) 2D-Linear Interpolation (data REs)
Equalization	Zero Forcing (ZF)

within a distance called the stationarity distance (SD). For A2G channels, extensive channel measurements in [10], [11] have shown that the SD ranges between 10 and 35 m. For a UAV traveling at an average speed of 75 m/s this corresponds to a stationarity time of up to 450 ms.

#### A. Scenario

We consider a scenario where a UAV is communicating with a ground station (GS) using an OFDM (LTE or NR-like) PHY layer (Table I). The scenario consists of three stages, each lasting for about 2 minutes:

- Stage 1: The UAV flies in a hilly section towards a city. Due to reflections from hills, there is a presence of strong multipath components ( $\tau_{rms} \sim 1\mu s$  [11]), and the UAV decelerates from 300 km/h to 200 km/h.
- Stage 2: The UAV then enters the suburban section, where  $\tau_{rms}$  fluctuates between 50 ns and 500 ns [10]. The UAV uniformly decelerates from 200 km/h to 100 km/h.
- Stage 3: The UAV enters the urban section, where the contributions of multipath become prominent due to the presence of tall buildings [10]. The UAV velocity decelerates further to 50 km/hr.

TABLE II: Codebook of Channel Profiles,  $\mathcal{R}_C$

$\mathcal{R}_{C,t}$ : Channel profiles for Doppler Frequency

Index ( $m$ )	Mobility Type	Velocity	$f_d^\dagger$ (Hz)
1	Almost stationary	1 km/h	4.6
2	Low speed (taxiing)	15 km/h	70
3	High speed (taxiing)	55 km/h	250
4	Takeoff/Landing	120 km/h	550
5	Medium speed (airborne)	160 km/h	750
6	High Speed (airborne)	250 km/h	1150

$^\dagger$ Doppler frequency for a center frequency of  $f_c = 5$  GHz.

$\mathcal{R}_{C,f}$ : Channel profiles for Power Delay Profiles (PDP)

Index ( $l$ )	Type of Scattering	$\tau_{rms}$
1	Low (near-LoS)	221.5
2	Medium (Suburban air-to-ground)	476.4
3	High (Near-Urban air-to-ground)	791.2
4	Very High (Urban/Hilly air-to-ground)	1440

Regulations or UAV mission may be the cause for the varying UAV speeds, for e.g. a package delivery mission. The maximum doppler frequency  $f_{d,m}$  is related to the velocity  $v$  by  $f_{d,m} = v f_c / c$ , where  $c$  is the velocity of light and  $f_c$  the carrier frequency. The SNR varies with distance based on the pathloss model parameters shown in Table I, using the distance-based path loss with log-Normal shadow fading [10]

$$PL(d) = A + 10n \log(d/R_{min}) + X - F \text{ [dB]}, \quad (6)$$

where  $R_{min} \leq d \leq R_{max}$  and  $X[\text{dB}] \sim \mathcal{N}(0, \sigma_X^2)$ .

#### B. Performance Comparison with Fixed Pilot Configurations

We compare our rate-maximizing pilot scheme to the fixed pilot configurations  $\mathcal{V}_{2,2}, \mathcal{V}_{4,2}, \mathcal{V}_{6,4}$  (similar to LTE),  $\mathcal{V}_{6,6}$  and  $\mathcal{V}_{8,8}$ , where  $\mathcal{V}_{a,b} = \{\rho, \Delta_p f, \Delta_p t\} = \{-3 \text{ dB}, a, b\}$ . Table II shows the channel statistics codebook  $\mathcal{R}_C$  with  $N_{\Delta f} = 62$  and  $N_{\Delta t} = 40$ , which is designed to cover most of the PDP and Doppler profiles. The pilot configuration  $\mathcal{V}$  takes values from the following:

- 1)  $\mathcal{P} = \{-10 \text{ dB}, -9 \text{ dB}, -7 \text{ dB}, -5 \text{ dB}, -3 \text{ dB}, 0 \text{ dB}\}$ .
- 2)  $\mathcal{D}_f = \{2, 4, \dots, 10, 12\}$ .
- 3)  $\mathcal{D}_t = \{1, 2, \dots, 9, 10\}$ .

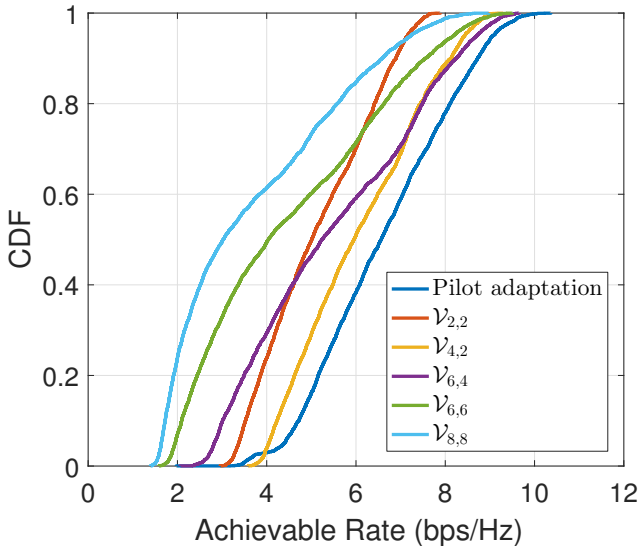


Fig. 4: CDF comparison of the average achievable rate of pilot adaptation scheme versus fixed pilot configuration schemes.

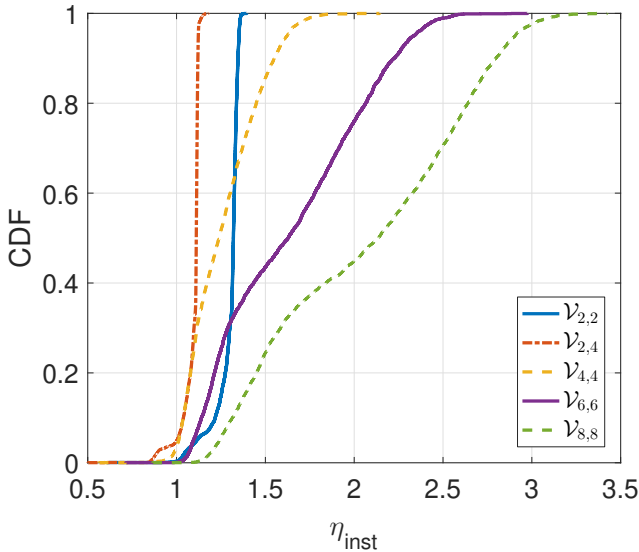


Fig. 5: CDF comparison of the instantaneous rate gain of pilot adaptation scheme versus fixed pilot configuration schemes.

Typically, the feasible sets should be chosen such that (a)  $\rho$  satisfies the PAPR requirements, (b)  $\Delta_p t$  is able to capture the channel variations accurately enough for a large range of vehicular velocities, and (c)  $\Delta_p f$  gives reasonably accurate channel estimates for a wide range of multipath environments. In order to estimate the optimal pilot configuration, we use  $T_{ofdm} = 1500$  OFDM symbols across  $N_{sub} = 72$  subcarriers to implement Algorithm 1. For this case the time duration between the estimation and the use of  $\mathcal{V}_o$  is 200 ms, which is less than the stationarity interval of 450 ms.

Fig. 4 shows the cumulative distribution function (CDF) of the achievable rates for all considered pilot configurations. We observe that our proposed adaptive pilot configuration

outperforms all the other fixed pilot schemes considered, with the average throughput gain ranging from 9% to 80%. Fig. 5 shows the CDF of the ratio of the instantaneous rates ( $\eta_{inst}$ ) obtained by the adaptive pilot configuration w.r.t. each considered fixed configuration. Table III shows the comparison of different percentile values of instantaneous rate gain, with  $\Delta\eta_{inst}^{(x\%)}$  representing the  $x$ -percentile rate gain. We observe that due to the high Doppler frequencies, the throughput performance deteriorates with higher values of  $\Delta_p t$ . Even compared to a high pilot density configuration such as  $\mathcal{V}_{2,2}$  and  $\mathcal{V}_{4,2}$  the proposed pilot adaptation procedure has rate gains ranging from 3.6% to 34.6%, demonstrating its efficacy.

The feedback overhead for explicit and implicit feedback mechanisms is  $\lceil \log_2(6 \times 6 \times 10) \rceil / (1500 \times 71.875 \mu s) = 83.5$  bps and  $\lceil \log_2(6 \times 4) \rceil / (1500 \times 71.875 \mu s) = 46.4$  bps respectively. Both of these values are negligible compared to the data rates supported by current wireless networks.

TABLE III: Instantaneous rate gains of adaptive pilot over fixed pilot configurations

Scheme	$\Delta\eta_{inst}^{(10\%)}$	$\Delta\eta_{inst}^{(50\%)}$	$\Delta\eta_{inst}^{(90\%)}$
$\mathcal{V}_{2,2}$	21.8%	32%	34.6%
$\mathcal{V}_{4,2}$	3.8%	11.1%	12%
$\mathcal{V}_{6,4}$	3.6%	23.9%	54.9%
$\mathcal{V}_{6,6}$	14%	62.8%	122.4%
$\mathcal{V}_{8,8}$	31.5%	113.6%	179.7%

## V. CONCLUSIONS

In this paper, we proposed an adaptive pilot configuration mechanism for A2G UAV communications. The receiver estimates channel statistics, maps them to a codebook, finds the optimal parameters and explicitly feeds them back to the transmitter. We compared its throughput performance against several fixed pilot configurations in a scenario where the channel statistics vary over time because of natural variations in the UAV flight environment and speed. We demonstrated average rate gains ranging from 9% to 80%, and median instantaneous rate gains ranging from 11% to 114%. The signaling feedback overhead for the proposed adaptive pilot configuration method is negligible. It provides a means to accommodate more users for 5G in densely populated UAV networks. For future research, the design of optimal resource allocation algorithms built around this framework is a natural extension to leverage the PHY layer gains of pilot adaptation.

## REFERENCES

- [1] Z. Xue, J. Wang, Q. Shi, G. Ding, and Q. Wu, "Time-Frequency Scheduling and Power Optimization for Reliable Multiple UAV Communications," *IEEE Access*, vol. 6, pp. 3992–4005, 2018.
- [2] H. He, S. Zhang, Y. Zeng, and R. Zhang, "Joint Altitude and Beamwidth Optimization for UAV-Enabled Multiuser Communications," *IEEE Commun. Lett.*, vol. 22, no. 2, pp. 344–347, Feb 2018.
- [3] J. Kakar and V. Marojevic, "Waveform and Spectrum Management for Unmanned Aerial Systems beyond 2025," in *Proc. IEEE International Symposium on Personal, Indoor and Mobile Radio Communications (PIMRC)*, October 2017.
- [4] M. Simko, P. S. Diniz, Q. Wang, and M. Rupp, "Adaptive pilot-symbol patterns for MIMO OFDM systems," *IEEE Trans. Wireless Commun.*, vol. 12, no. 9, pp. 4705–4715, 2013.

- [5] R. M. Rao, V. Marojevic, and J. H. Reed, "Adaptive Pilot Patterns for CA-OFDM Systems in Nonstationary Wireless Channels," *IEEE Trans. Veh. Technol.*, vol. 67, no. 2, pp. 1231–1244, Feb 2018.
- [6] 3GPP, "Physical channels and modulation (Release 15)," 3rd Generation Partnership Project (3GPP), TS 38.211, Dec. 2017. [Online]. Available: <http://www.3gpp.org/dynareport/38211.htm>
- [7] B. Yang, K. B. Letaief, R. S. Cheng, and Z. Cao, "Channel Estimation for OFDM Transmission in Multipath Fading Channels Based on Parametric Channel Modeling," *IEEE Trans. Commun.*, vol. 49, no. 3, pp. 467–479, Mar 2001.
- [8] Y. Li and L. J. Cimini, "Bounds on the Interchannel Interference of OFDM in Time-varying Impairments," *IEEE Trans. Commun.*, vol. 49, no. 3, pp. 401–404, 2001.
- [9] T. Cui and C. Tellambura, "Power delay profile and noise variance estimation for OFDM," *IEEE Commun. Lett.*, vol. 10, no. 1, pp. 25–27, Jan 2006.
- [10] D. W. Matolak and R. Sun, "Air-Ground Channel Characterization for Unmanned Aircraft Systems—Part III: The Suburban and Near-Urban Environments," *IEEE Trans. Veh. Technol.*, vol. 66, no. 8, pp. 6607–6618, Aug 2017.
- [11] R. Sun and D. W. Matolak, "Air-Ground Channel Characterization for Unmanned Aircraft Systems Part II: Hilly and Mountainous Settings," *IEEE Trans. Veh. Technol.*, vol. 66, no. 3, pp. 1913–1925, March 2017.